Avoidance of Constant Velocity Targets Using Bearing and Time-to-Collision

James J. Adams, Jen Jui Liu, and Randal W. Beard

Abstract—This paper address the problem of path deconfliction and collision avoidance for unmanned aerial vehicles equipped with a monocular optical camera. The measurements observed from the camera do not include range, but they do allow for calculation of time-to-collision. In this paper we exploit the idea that a single time-to-collision estimate may have come from any number of intruders with different range and velocities, to define a family of potential intruders. The family of potential intruders is represented by a set of particles that can then be propagated forward in time to represent the set of all potential collision scenarios. A path planning algorithm is then introduced to minimize the collision risk. The method is illustrated with simulation results.

I. INTRODUCTION

Path deconfliction and collision avoidance is a critical capability for autonomous systems [1]. It is essential for autonomous systems operating in various environments, including urban cities with heavy air traffic and remote regions with unpredictable terrain. Unmanned aerial vehicles (UAVs) need to be able to detect and avoid obstacles in the environment to ensure safe and effective navigation.

Critical to the problem of collision avoidance is estimation of the intruder pose. Use of LiDAR and radar for estimation is very effective due to their ability to directly measure range to the intruder [2]. However, these systems are usually large or have a very narrow field of view. Monocular optical cameras are a much more desirable sensor for small UAVs due to their inexpensive, lightweight nature. The lack of range information from these cameras represents a major challenge to their utilization in intruder pose estimation as they can only provide bearing measurements and rates of expansion of the target in the camera image.

Pose estimation of a moving target using a single maneuvering, bearing-only sensor has been extensively researched and analyzed [3], [4], [5], [6]. According to theoretical results, the target state remains unobservable until certain conditions are met. In order to detect a target accurately, the sensor's motion must be at least one order higher than the target's motion. For instance, if a target is moving at a constant velocity, the observer must at least move with constant, nonzero acceleration [5] though other maneuvers also make the targets pose observable.

*This work was supported by Scientific Systems Company Inc, on the Open Autonomy/Safety Enhancement System (OASES), Subcontract No. SC-1754-01. In support of Prime Contract No. FA8649-22-P-0770

James J. Adams and Jen Jui Liu are graduate research assistants in the MAGICC Lab, Brigham Young University, Provo, USA (bmcc1745, jenjui.liu)@gmail.com

Randal W. Beard is a Professor in the Department of Electrical and Computer Engineering, Brigham Young University, Provo, USA, beard@byu.edu

In light of this, many different types of estimators have been proposed for use in bearing-only pose estimation of moving targets including extended Kalman filters, unscented Kalman filters, and Pseudo-Linear Kalman Filters (PLKF) [7], [8]. Each of these estimators can converge to the correct pose of the intruder given enough time and sufficiently strong self-maneuvers, with larger self-maneuvers generally corresponding to quicker convergence.

In some applications it is desirable for the ownship to maneuver as little as possible while avoiding collision with other aircraft. One such case is when engaging with other potentially cooperative aerial vehicles. In this case it is desirable to move with constant velocity until the avoidance maneuver is performed to avoid confusion. The estimators mentioned above would struggle with this requirement.

Research has shown that humans and insects use time-to-collision (TTC), calculated from the expansion rate of the target in the field of view, to maneuver in the environment, and its application to UAVs has also been studied [9], [10], [11]. We would like to incorporate this additional information into our method of estimation.

In light of the difficulties of target pose estimation with low-maneuvering observers and the additional information that can be obtained from camera sensors, we propose the application of a novel particle filter to the problem of intruder pose estimation. A path planning algorithm to navigate the ownship to an objective while minimizing the risk of collision is also presented. It is desirable to maintain constant altitude during avoidance maneuvers to comply with Visual Flight Rules [12]. Our methods are therefore derived for use in 2D, though no significant barrier exists to the extension of these methods into three dimensions.

II. TRAJECTORY FAMILIES

Time-to-collision (TTC), denoted by τ , is given by the equation

$$\tau = \frac{2\epsilon_A}{\dot{\epsilon}_A} = -\frac{(p_i(t) - p_o(t))^\top e_c}{(v_i - v_o)^\top e_c},\tag{1}$$

where ϵ_A and $\dot{\epsilon}_A$ are the area of the object in the camera frame in calibrated normalized pixel coordinates and its derivative, p_i and v_i are the position and velocity of the intruder, p_o and v_o are the position and velocity of the ownship, and e_c is the unit vector along the optical axis of the camera [13]. We assume that the position and velocity of the ownship is known, either by GPS or Visual Inertial Odometry. Equation (1) represents the amount of time in the future where a "collision" will occur, or when the distance

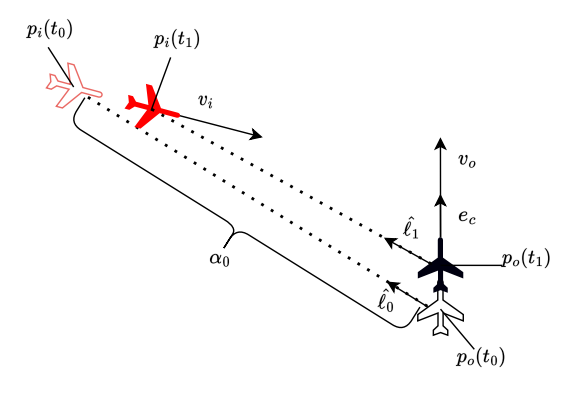


Fig. 1: The ownship and intruder at times t_0 and t_1 with line-of-sight vectors.

between the intruder and ownship along the camera optical axis will be zero. We define $t_c \triangleq \tau(t) + t$ to be the time of collision (TOC). If neither the ownship nor the intruder is accelerating, $\frac{d\tau}{dt} = -1$, and thus t_c is constant.

We now show that there is a family of constant velocity trajectories that all appear identical to the observer if the ownship follows a constant velocity trajectory. Let $p_d(t) = \gamma(p_i(t) - p_o(t)) + p_o(t)$ where $\gamma > 0$ is a constant. Differentiating we obtain $\dot{p}_d(t) = \gamma(v_i - v_o) + v_o \triangleq v_d$, which is constant. Therefore so $p_d(t)$ is a constant velocity trajectory. Letting $\hat{\ell}_i$ and $\hat{\ell}_d$ be the unit vectors from p_o to p_i and p_d , respectively, we have that

$$\begin{split} \hat{\ell}_d &= \frac{p_d(t) - p_o(t)}{||p_d(t) - p_o(t)||} = \frac{\gamma(p_i(t) - p_o(t))}{||\gamma(p_i(t) - p_o(t))||} \\ &= \frac{p_i(t) - p_o(t)}{||p_i(t) - p_o(t)||} = \hat{\ell}_i, \end{split}$$

which implies that the unit vectors from p_o to p_d and from p_o to p_i are identical at any given time. Similarly, let τ_i and τ_d be the time-to-collision of the two trajectories, then

$$\tau_{d} = \frac{(p_{d}(t) - p_{o}(t))^{\top} e_{c}}{(v_{o} - v_{d})^{\top} e_{c}} = \frac{\gamma (p_{i}(t) - p_{0}(t))^{\top} e_{c}}{\gamma (v_{o} - v_{i})^{\top} e_{c}}$$
$$= \frac{(p_{i}(t) - p_{o}(t))^{\top} e_{c}}{(v_{o} - v_{i})^{\top} e_{c}} = \tau_{i},$$

which implies that the time-to-collision measurement associated with the two trajectories will be identical, and therefore the two trajectories $p_i(t)$ and $p_d(t)$ will appear identical to the ownship if the ownship follows a constant velocity trajectory. By varying γ it is possible to construct the family of trajectories to which the intruder belongs, assuming we have an example trajectory on which to base the family.

It has been well established in the literature on bearingonly estimation that the full pose of an intruder is only observable if the ownship outmaneuvers the intruder [4], [5]. In this case where the intruder is moving with constant velocity, the ownship must accelerate for the pose to be observable. As we have shown there are multiple unique constant velocity trajectories that appear identical to the ownship observer, the introduction of TTC does not make the full pose of the intruder observable, but the use of TTC can greatly improve our estimate of the target velocity.

We now present a strategy to find the velocity of an intruder given its range. Let $\hat{\ell}_0$ and $\hat{\ell}_1$ be the bearing measurements at times t_0 and t_1 , respectively. At time t_0 , the target must lie along the unit vector $\hat{\ell}_0$ from the position of the ownship at that time. We write this constraint as

$$p_i(t_0) = p_o(t_0) + \alpha_0 \hat{\ell}_0 \tag{2}$$

where α_0 is the range to the intruder at time t_0 . Similarly, at time t_1 the target must be along the unit vector $\hat{\ell}_1$ from the position of the ownship, and we can write

$$p_i(t_1) = p_o(t_1) + \alpha_1 \hat{\ell}_1 \tag{3}$$

Assuming the intruder and ownship move with constant velocity, we can rewrite Equation (3) as

$$p_i(t_0) + v_i(t_1 - t_0) = p_o(t_1) + \alpha_1 \hat{\ell}_1. \tag{4}$$

Since we do not assume that the intruder is on a collision course with the ownship, the vectors $\hat{\ell}_0$ and $\hat{\ell}_1$ are not necessarily equal.

At time t_c , the quantity $\tau = \frac{(p_i - p_o)^\top e_c}{(v_o - v_i)^\top e_c} = 0$, and so $(p_i(t_c) - p_o(t_c))^\top e_c = 0$. In the 2D case, this means the quantity $p_i(t_c) - p_o(t_c)$ lies along the unit vector perpendicular to e_c (we denote this as e_c^\perp), which we will write as follows

$$p_i(t_c) - p_o(t_c) = \alpha_\tau e_c^\perp \tag{5}$$

Again assuming constant velocity motion, we rewrite Equation (5) as

$$p_i(t_0) + v_i(t_c - t_0) - p_o(t_c) = \alpha_\tau e_c^\perp$$
 (6)

Writing equations (4) and (6) in matrix form gives

$$\underbrace{\begin{bmatrix} -\hat{\ell}_{1} & 0 & (t_{1} - t_{0})I_{2\times 2} \\ 0 & -e_{c}^{\perp} & (t_{c} - t_{0})I_{2\times 2} \end{bmatrix}}_{A} \underbrace{\begin{bmatrix} \alpha_{1} \\ \alpha_{\tau} \\ v_{i} \end{bmatrix}}_{x} = \underbrace{\begin{bmatrix} p_{o}(t_{1}) - p_{i}(t_{0}) \\ p_{o}(t_{c}) - p_{i}(t_{0}) \end{bmatrix}}_{b}$$
(7)

Taken together with equation (2), this set of equations can thus give us the velocity of the target for any given initial range α_0 .

We can continue to add bearing measurements as desired to generalize equation (7) for many bearing measurements:

$$\underbrace{\begin{bmatrix}
-\hat{\ell}_{1} & 0 & \cdots & 0 & 0 & (t_{1} - t_{0})I_{2 \times 2} \\
0 & -\hat{\ell}_{2} & \cdots & 0 & 0 & (t_{2} - t_{0})I_{2 \times 2} \\
\vdots & \vdots & \ddots & \vdots & \vdots & \vdots \\
0 & 0 & \cdots & -\hat{\ell}_{n} & 0 & (t_{n} - t_{0})I_{2 \times 2} \\
0 & 0 & \cdots & 0 & -e_{c}^{\perp} & (\bar{t}_{c} - t_{0})I_{2 \times 2}
\end{bmatrix}}_{A} \underbrace{\begin{bmatrix}
\alpha_{1} \\ \alpha_{2} \\ \vdots \\ \alpha_{n} \\ \alpha_{\tau} \\ v_{i}
\end{bmatrix}}_{x} = \underbrace{\begin{bmatrix}
p_{o}(t_{1}) - p_{i}(t_{0}) \\
p_{o}(t_{2}) - p_{i}(t_{0}) \\
\vdots \\
p_{o}(t_{n}) - p_{i}(t_{0}) \\
p_{o}(\bar{t}_{c}) - p_{i}(t_{0})
\end{bmatrix}}_{x} (8)$$

where \bar{t}_c is the average TOC found from the TTC measurements. Adding more measurements can give us a better estimate of the velocity given the noise-corrupted nature of the measurements.

The meaning of the TTC measurements becomes less clear when the ownship is accelerating, but dropping the last line of equation (8) would allow us to obtain a velocity estimate even if the ownship is accelerating, and this works better the greater the time difference between the first and last bearing measurements. In fact, the $p_i(t_0)$ variable could be moved to the left side of the equation and doing sowould in theory allow us to invert A to obtain the full pose of the intruder. In practice the matrix A is singular if the ownship is not accelerating and very close to singular unless major maneuvers are performed. It is thus not useful for practical application aside from velocity estimation.

We can then constrain the family of possible trajectories based on a minimum and maximum detection range $(r_{min}$ and $r_{max})$, as well as a maximum expected speed. From these constraints we can obtain an γ_{min} and γ_{max} to bound the family of trajectories. Figure 2 shows some examples of various trajectory families, with the blue line representing the actual intruder trajectory, the red line representing the ownship trajectory, and the green and orange lines representing the γ_{max} and γ_{min} trajectories, respectively.

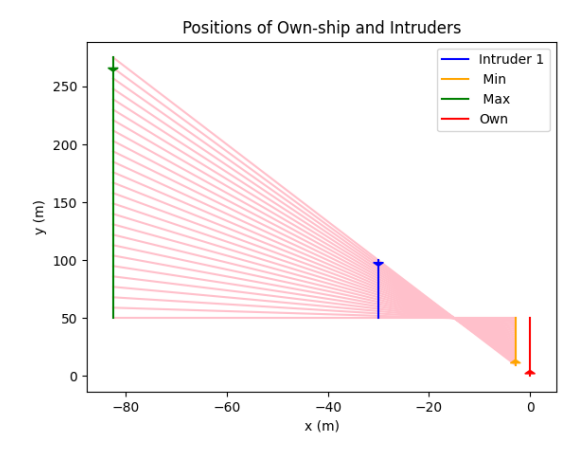
III. PARTICLE FILTER

The standard approach to the particle filter is the Sample Importance Resampling (SIR) method. In this scenario, the particles would be initialized with a random position along the first bearing measurement and a random velocity. At each timestep the particles are weighted by how well they match the current measurement, with new particles generated from the highest weighted particles [14].

However, an SIR particle filter has many disadvantages when applied to the problem addressed in this paper. First, the velocity space for a given particle to match the behavior of the intruder we wish to approximate is very small. Thus, creating particles with a random velocity produces very few feasible trajectories. An infeasibly large number of particles would need to be generated to produce valid particles over all possible ranges.

The second disadvantage is the nature of the bearing measurement. These measurements tightly constrain lateral position when the intruder is close, but this constraint loosens as range increases. This tight constraint at close ranges means that small perturbations in the random resampling of particles close to the ownship tend to have a larger impact on the subsequent weight of the particle compared to distant particles. Scaling the perturbations based on range to the particle does little to negate this issue. The effect is that particles close to the ownship are filtered out at a much greater rate than those far away, leading to a skew in range estimation away from the ownship.

This paper proposes a new approach to particle sampling for this problem. Namely, the velocity of the particles are determined using the current TOC and bearing measurements.



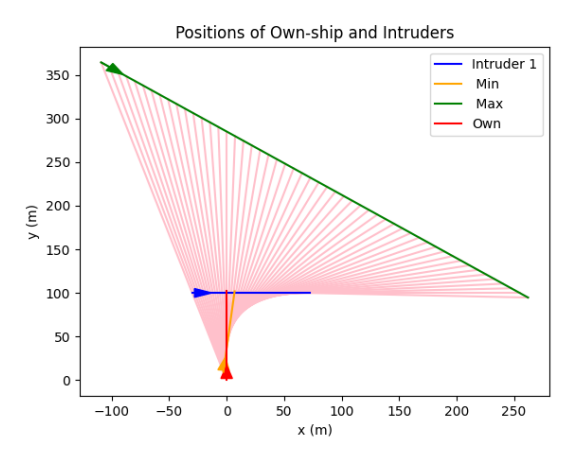


Fig. 2: Examples of trajectory families generated by various intruder behaviors, with (a) being produced by the intruder passing on the left, and (b) being produced by the intruder passing in front of the ownship.

This method produces particles with behavior that better matches the intruder. The method of updating the particles can also be changed to estimate the range of the intruder as it becomes observable as the ownship maneuvers.

A. Initialization of Particles

After tracking of the object has begun and two bearing and one TOC measurement have been made, the particles are initialized. This method of particle initialization aims to fill the potential position space as thoroughly as possible. Let $\hat{\ell}_0$ and $\hat{\ell}_1$ be the two bearing measurements, and t_c be the TOC measurement. Let $R(\theta)$ be the rotation matrix that rotates a vector in the 2D plane by θ . The range is randomly selected from between the minimum and maximum possible values: $\alpha_0^{[m]} \sim \mathcal{U}(\gamma_{min}, \gamma_{max})$. The bearing vector is then rotated by a random amount: $\hat{\ell}_0^{[m]} = R(\theta_0)\hat{\ell}_0$ and $\hat{\ell}_1^{[m]} = R(\theta_1)\hat{\ell}_1$ where $\theta_0, \theta_1 \sim \mathcal{N}(0, \sigma)$. The TOC measurement is also augmented: $\tilde{t}_c^{[m]} \sim \mathcal{N}(t_c, \sigma_\tau)$. The initial position is then given by $p_i^{[m]}(t_0) = p_o(t_0) + \alpha_0 \tilde{\ell}_0^{[m]}$, and these modified values are then input into Equation (8) to obtain the particle velocity $v_i^{[m]}$. This initialization process produces particles with both range diversity and feasible velocities.

B. Measurement Update

The method of updating the particle filter depends on whether or not the ownship has accelerated in the time between the last measurement. If no acceleration has occurred, the measurement update roughly follows an SIR update. From the most recent TTC measurement we can obtain a new TOC estimate $t_{c,k} = \tau(t_k) + t_k$, which is averaged with previous estimates to eliminate noise:

$$\bar{t}_c = \frac{1}{k} \sum_{i=1}^k t_{c,i} \tag{9}$$

The position of the particles at the current time t_k is calculated using their initial position and calculated velocity: $p_i^{[m]}(t_k) = p_i^{[m]}(t_0) + v_i^{[m]}t_k$. The particles are then weighted by how closely their LOS vector matches that of the bearing measurement using

$$w_k^{[m]} = \frac{1}{W_k} exp(-\frac{1}{2}(h(x_k^{[m]}) - \hat{\ell}_k)^{\top} R^{-1}(h(x_k^{[m]}) - \hat{\ell}_k)),$$
(10)

where $\hat{\ell}_k$ is the bearing measurement at time t_k , W_k is the total weight of all the particles,

$$h(x_k^{[m]}) = \frac{p_i^{[m]}(t_k) - p_o(t_k)}{||p_i^{[m]}(t_k) - p_o(t_k)||}$$
(11)

is the measurement function, and $R = \text{Diag}(\sigma_x, \sigma_y)$. The particles are then re-sampled according to this new weighting, with random perturbations made to the initial locations of the particles. This new initial location is then taken with the previous LOS vectors and the averaged TOC and substituted into equation (8) to produce the best estimate of the velocity of the particle.

In the case that the ownship is accelerating, the measurement update is simply used to weight the particles. The number of effective particles can be calculated as

$$N_{\text{eff}} = \frac{N}{1 + \text{var}(w_k)} \tag{12}$$

where N is the total number of particles. The particles are resampled if $N_{\rm eff}$ falls below a certain threshold. This more closely follows existing PF applications to bearing-only pose estimation with ownship maneuvers [15].

C. Utilization in Path Planning

As the velocity of the particles is known from the updates, their positions at a future timestep can be predicted. These predicted positions essentially sample the probability distribution at the given time, and so a probability density function can then be fit to the particles using a kernel-density estimate (KDE). For our application we use a Gaussian KDE to estimate the probability density function. These PDFs, denoted as $P_i(t_k,x)$ in the subsequent section, are then used in the path planning algorithm to find an optimal path to avoid the potential locations of the intruder.

IV. B-SPLINE BASED PATH PLANNING ALGORITHM

In this section we present a path planner that utilizes continuous B-splines to avoid areas with high collision probability. The objective function and constraints are used to optimize the path by minimizing the path's cost while satisfying the constraints. Our objective is to navigate the ownship from its start position to a specified end position taking the shortest path while avoiding the locations where the intruder has a high probability of occupying. The objective function

$$J(\mathbf{c}) = ||c_L - p_a|| \tag{13}$$

penalizes the distance between the goal location $p_g \in \mathbb{R}^2$ and the last control point $c_L \in \mathbb{R}^2$, where $\mathbf{c} = (c_1, \dots, c_L) \in \mathbb{R}^{2 \times L}$ are the B-spline control points. Since the velocity of B-spines is a function of the difference between control points, the constraints

$$v_{min} \le \frac{||c_k - c_{k+1}||}{\Delta t} \le v_{max} \tag{14}$$

limit the velocity between any control point and the next control point. When the ownship is a multirotor and can therefore hover or stop, v_{min} is zero.

The probability distribution of the ownship is denoted by

$$\begin{split} P_o(t, x) &\sim \mu_o \exp{[-\frac{1}{2}(x - p_o(t))^{\top} \Sigma_o^{-1}(t)(x - p_o(t))]} \\ &= \mathcal{N}(p_o(t), \Sigma_o(t)) \end{split}$$

while the probability distribution of the intruder is denoted by $P_i(t,x)$. It is important to note that there may be multiple intruders, and in that case $P_i(t,x)$ will be the convex sum of the individual probability distributions. Lastly, $P_o(t_k,c_k)$ refers to the ownship's probability distribution at a specific control point, denoted by c_k , at time t_k .

By the multiplication law of conditional probability, the collision probability is $P_c(t,x) = P_i(t,x)P_o(t,x)$ If P_{max} denotes the maximum allowed collision probability, then we require that for all $x \in S$

$$P_c(t,x) = P_o(t,x)P_i(t,x) \le P_{max}.$$

Since B-spline paths are contained in the convex hull of local control points, we constrain the collision probability at the control points:

$$P_o(t_k, c_k)P_i(t_k, c_k) \le P_{max}, \ k = 1, \dots, L,$$
 (15)

where $P_i(t,x)$ is computed using the particle filter described in the previous section, and where Equation (14) ensures that the control points remain closely spaced avoiding the case where most of the probability mass of $P_i(t_k,x)$ would be in the local convex hull of the control points.

We begin the optimization by setting all control points equal the current position of the ownship $x_0 = p_s$. Such initial settings help the control points to avoid infeasible regions. It is also intuitive to generate the path from the starting position to the goal.

In our implementation, we used the Python/Scipy/Optimization library with settings

```
scipy.optimize.minimize(
   objective_function,
   X0,
   method='SLSQP',
   bounds=None,
   constraints=[nlc_1, nlc_2])
```

where objective_function is the objective function given by Equation (13), X0 is the initial control point locations which we set to be the current ownship position, and where nlc_1, nlc_2 are the constraints given in Equations (14) and (15).

V. RESULTS

In this section we present two simulation results of collision avoidance using our algorithm. In both of these examples the goal location is directly in front of the ownship. In our implementation we continue to fly with constant velocity for about 1 second after the initial intruder detection to allow the particle filter to converge before planning an avoidance path. Therefore, in these simulations, the predicted path of the particles and the path planned for the ownship only take into consideration information derived during one second of constant velocity flight.

Figure 3 illustrates planning results for one intruder and Figure 4 illustrates planning results for two intruders. The "time" bar in these plots represents time in the future as measured from the current time. The large red dot represents the future position of the ownship if it follows the planned path, and the large orange and green dots are the actual future positions of the intruders if the continue to follow constant velocity trajectories. The small blue dots are the particle filter positions projected into the future.

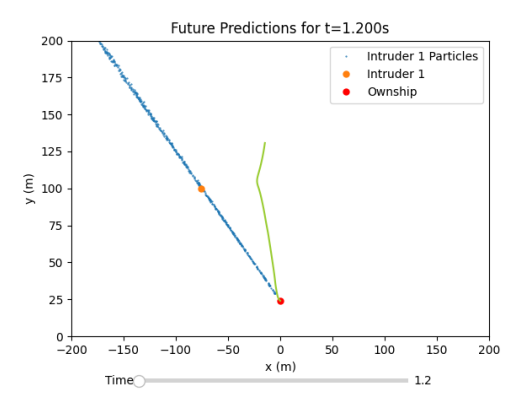
In Figure 3, the ownship must maneuver to avoid the intruder. It does so and avoids collision with the densest region of particles and therefore avoids the actual intruder. In Figure 4, small manuevers result in a collision-free path. From these examples we see that our method is able to avoid collision with multiple intruders while maneuvering only when required, and using only bearing and time-to-collision measurements that are readily available from a camera.

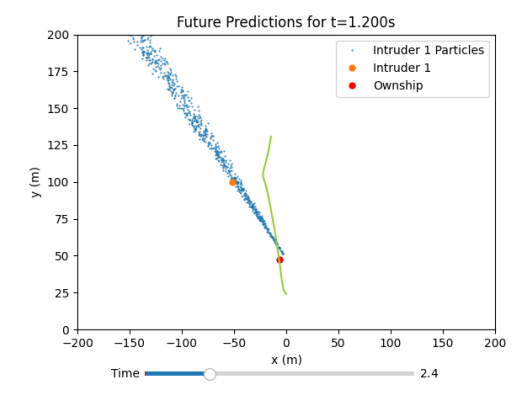
VI. CONCLUSION

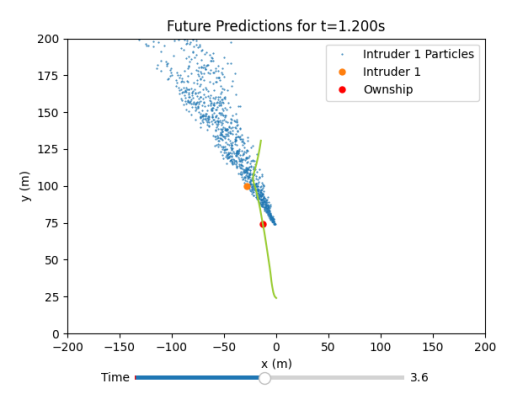
In this paper we have developed a new approach to intruder pose estimation utilizing only information obtained from a monocular optical camera, namely bearing and time-to-collision. We have also developed a path planning algorithm that maneuvers the ownship toward an objective while minimizing the risk of collision.

Results indicate that our method is effective in approximating the family to which the intruder belongs without the need for self-maneuvering. This method also produces trajectories that avoid the areas with highest probability of occupation while driving the ownship toward its objective. An advantage of our approach is that the pose of an intruder can continue to be estimated as the ownship begins to maneuver.

Future work includes improved initialization of the particles. The initialization of the particle filter requires the







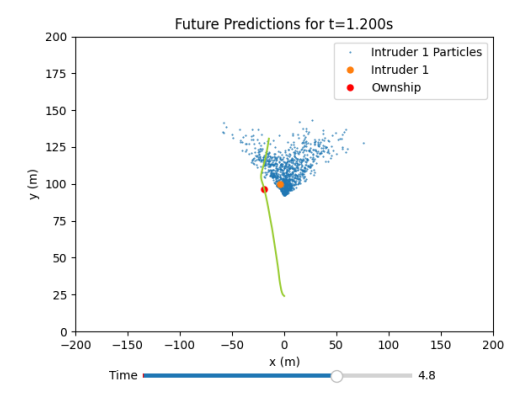
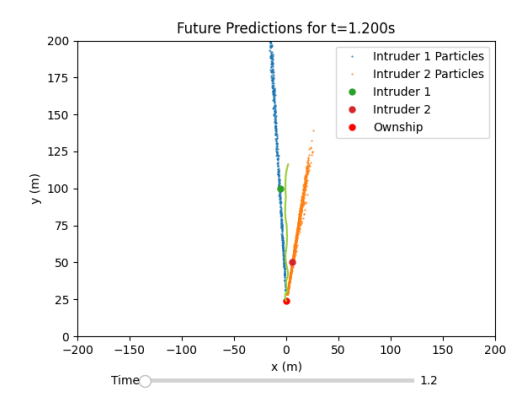
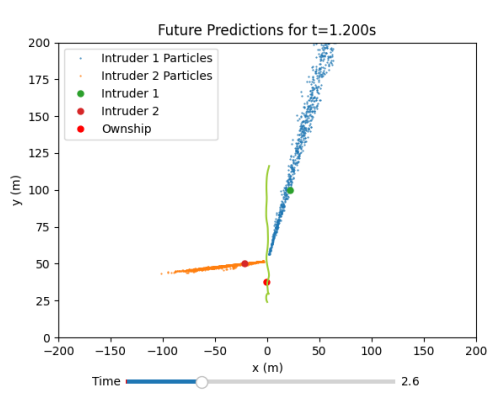
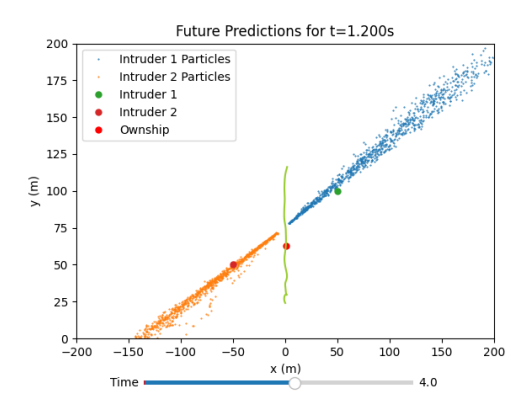


Fig. 3: Avoidance of Intruder on Direct Collision Course







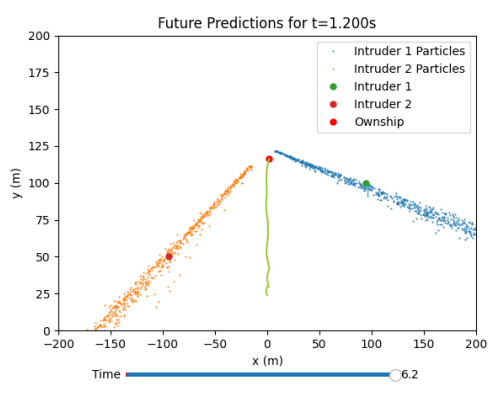


Fig. 4: Avoidance of two intruders on near-miss trajectories.

ownship to not maneuver during the first two measurements. While this requirement is likely to be met in all but the busiest airspaces, the elimination of this requirement would improve the robustness of the method.

Additional improvement is also needed in the path planning algorithm. One possible way to improve the efficiency of the planning would be to utilize an RRT-like method to generate a feasible trajectory through the probability fields from which a B-Spline trajectory can then be generated.

REFERENCES

- J. Borenstein and Y. Koren, "Real-time obstacle avoidance for fast mobile robots," *IEEE Transactions on Systems, Man, and Cybernetics*, vol. 19, pp. 1179–1187, 1989.
- [2] X. Liu, C. Yuan, and F. Zhang, "Targetless extrinsic calibration of multiple small fov lidars and cameras using adaptive voxelization," *IEEE Transactions on Instrumentation and Measurement*, vol. 71, pp. 1–12, 9 2022.
- [3] V. J. Aidala and S. E. Hammel, "Utilization of modified polar coordinates for bearings-only tracking," *IEEE Transactions on Automatic Control*, vol. 28, pp. 283–294, 3 1983.
- [4] E. Fogel and M. Gavish, "Nth-order dynamics target observability from angle measurements," *IEEE Transactions on Aerospace and Electronic Systems*, vol. 24, pp. 305–308, 5 1988.
- [5] G. C. Carter, "A brief description of the fundamental difficulties in passive ranging," *IEEE Journal of Oceanic Engineering*, vol. 3, pp. 65–66, 5 1978.
- [6] R. R. Allen and S. S. Blackman, "Angle-only tracking with a msc filter," 1991, pp. 561–566.
- [7] J. Li, Z. Ning, S. He, C. H. Lee, and S. Zhao, "Three-dimensional bearing-only target following via observability-enhanced helical guidance," *IEEE Transactions on Robotics*, 4 2023.
- [8] K. S. Divya, S. K. Rao, K. S. Ramesh, and G. N. Divya, "Application of particle filter for passive underwater bearing only tracking." Institute of Electrical and Electronics Engineers Inc., 2021, pp. 1822– 1827.
- [9] W. E. Green and P. Y. Oh, "Optic-flow-based collision avoidance: Applications using a hybrid MAV," *IEEE Robotics and Automation Magazine*, vol. 15, pp. 96–103, 2008.
- [10] D. N. Lee, "A theory of visual control of braking based on information about time-to-collision," *Perception*, vol. 5, pp. 437–459, 1976.
- [11] M. Egelhaaf, "Optic flow based spatial vision in insects," Journal of Comparative Physiology A: Neuroethology, Sensory, Neural, and Behavioral Physiology, vol. 209, pp. 541–561, 7 2023.
- [12] H. Alturbeh and J. F. Whidborne, "Visual flight rules-based collision avoidance systems for UAV flying in civil aerospace," *Robotics*, vol. 9, 3 2020.
- [13] R. W. Beard, Vision-Based Estimation and Control of Multirotor and Winged-VTOL Systems. Brigham Young University, 4 2023. [Online]. Available: https://github.com/randybeard/vtolbook
- [14] K. Heine, "Unified framework for sampling/importance resampling algorithms," 2005, pp. 1459–1464.
- [15] X. Lin, T. Kirubarajan, Y. Bar-Shalom, and S. Maskell, "Comparison of EKF, pseudomeasurement, and particle filters for a bearing-only target tracking problem," *Signal and Data Processing of Small Targets*, vol. 4728, pp. 240–250, 8 2002.